Journal of the Korean Nuclear Society
Volume 30, Number 2, pp.128~139, April 1998

Effect of UO_2 Powder Property and Oxygen Potential on Sintering Characteristics of UO_2-Gd_2O_3 Fuel

Kun Woo Song, Keon Sik Kim, Ho Sik Yoo, and Youn Ho Jung
Korea Atomic Energy Research Institute
150 Dukjin-dong, Yusong-gu, Taejon 305-353, Korea

(Received November 4, 1997)

Abstract

The effect of UO_2 powder property and oxygen potential on characteristics of sintered UO_2-Gd_2O_3 fuel pellets has been investigated. Two types of powder, mixture of AUC-UO_2 and Gd_2O_3 powders (type I) and mixture of ADU-UO_2 and Gd_2O_3 powders (type II), have been prepared, pressed, and sintered at 1680℃ for 4 hours. Four sintering atmospheres with different mixing ratios of CO_2 to H_2 gas ranging from 0 to 0.3 have been used. UO_2-Gd_2O_3 fuel has lower sintered density than UO_2 fuel, and the density drop is larger for powder type I than for powder type II. As the oxygen potential increases, the sintered density of UO_2-2wt% Gd_2O_3 pellets increases but that of UO_2-10wt% Gd_2O_3 pellets decreases. It is found that pores are newly formed in UO_2-10wt% Gd_2O_3 pellets in accordance with the decrease in density. The grain size of UO_2-Gd_2O_3 fuel increases and a short range Gd distribution becomes homogeneous as the oxygen potential increases. A long range Gd distribution and grain structure are inhomogeneous for powder type II. The lattice parameter of $(U,Gd)O_2$ solid solution decreases linearly with Gd_2O_3 content. The dependence of UO_2-Gd_2O_3 fuel characteristics on powder type and sintering atmosphere have been discussed.

1. Introduction

A burnable absorber has been used to suppress initial excess reactivity at BOL (beginning of life) in LWRs. The UO_2 fuel pellet containing Gd_2O_3 has been widely used as a burnable absorber, in which the Gd2O3 content has been increasing to achieve extended fuel cycles. Currently, Gd_2O_3 contents of 8 to 10 wt% are not exceptional in PWRs. The UO_2-Gd_2O_3 fuel containing high Gd2O3 content is known to cause a sintering problem, in other words, it has low density and inhomogeneous microstructure under the sintering condition of pure UO_2 fuel pellets, compared with that containing low Gd_2O_3 content.

Recently, the fabrication of UO_2-Gd_2O_3 pellets has been studied to solve above problems in several investigations. Manzel and Doerr [1] studied the sintering kinetics of UO_2 and UO_2-4 wt% Gd_2O_3 in hydrogen, and reported that shrinkage of UO_2-4wt% Gd_2O_3 pellets was retarded by the formation of $(U,Gd)O_2$ solid solution. Ho and Radford [2] sintered UO_2-9 wt% Gd_2O_3 in dry, wet, and very wet hydrogen atmospheres, and reported that sintered density decreased as the oxygen potential of the sintering

atmosphere increased. They supposed that the defect complex made of both Gd ions and higher valent uranium ions hindered diffusion of uranium ions in high oxygen potential and consequently sintered density decreased. Recently, Yuda and Une [3] studied the sintering kinetics of UO_2-(5,10)wt% Gd_2O_3 in the mixture of CO and CO_2 gases, and found that sintered density decreased but Gd homogeneity increased as the oxygen potential of sintering atmosphere increased. They supposed that large pores formed in high oxygen potential cause the decrease in density. Riella et al. [4] studied the effect of powder preparations on the property of sintered UO_2-Gd_2O_3 pellets, which included the mixing of AUC-UO_2 with Gd_2O_3 powders and co-precipitation of (U,Gd)O_2 powder via AUC and ADU. They reported that the co-precipitation method yielded higher density and better Gd homogeneity. Therefore, oxygen potential and powder property are thought to be main sintering variables of UO_2-Gd_2O_3 fuel pellets.

This work has been undertaken to study the effect of oxygen potential and powder property on sintering characteristics of UO_2-Gd_2O_3 fuel. Sintered density, microstructure development and Gd homogeneity have been studied and correlated with sintering variables.

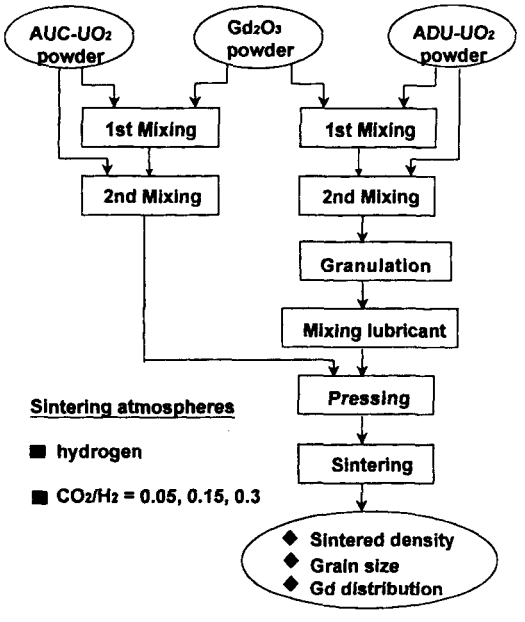

Fig. 1. Flow Diagram of Experimental Procedures

2. Experimental Procedures

Experimental procedures are shown in Fig. 1. Two types of UO_2 powder were used ; UO_2 powders through AUC (Ammonium Uranyl Carbonate) process and ADU (Ammonium Di-Uranate) process. The particle sizes of AUC-UO_2 powder and ADU-UO_2 powder were measured by a laser light scattering method, being about 19 ± 3 ㎛ and 2.2 ± 0.2 ㎛, respectively. The particle size of Gd_2O_3 powder was about 4.1 ± 0.4 ㎛. Other properties of the UO_2 powders have been described elsewhere [5,6]. Morphology of the UO_2 powders was observed with SEM.

When UO_2 powder was mixed with Gd_2O_3 powder, two-step mixing was carried out in order to get a homogeneous mixture. In the first mixing step, UO_2 powder was mixed with the same amount of Gd_2O_3 powder for 2 hours in so-called "Turbula", and in the second mixing step the mixture was diluted with additional UO_2 powder to meet a final composition and then mixed again for 2 hours. Three independent samples for chemical analysis were taken from the final powder mixture, and the differences between three gadolinium contents are less than 0.2 wt%. Final Gd_2O_3 contents in the mixed powders are 2, 5, 10 and 15% by weight. In this paper "power type I" stands for the mixed powder of AUC-UO_2 and Gd_2O_3 powders and "powder type II" for the mixed powder of ADU-UO_2 and Gd_2O_3 powders.

Powder type I is flowable enough to be pressed directly, but powder type II is little flowable so it needs granulation prior to direct-pressing. The powder type II was pre-pressed into slugs, which

were broken into granules. The zinc stearate was added to the mixed powders at the level of 0.2 wt% as a lubricant, and then mixed for 20 min in the Turbula. The prepared powder was pressed at 392 MPa(4 ton/cm^2) into green pellets, which have densities of 6.0±0.15 g/cm^3 for powder type I and 5.4±0.1 g/cm^3 for powder type II. The green pellet was heated to 700℃ and then held for 1 hour to burn the lubricant out. Subsequently it was heated to 1680℃, at which it was held for 4 hours prior to cooling. Four different sintering atmospheres were used in this work; pure hydrogen and mixtures of hydrogen (H_2) and carbon dioxide (CO_2) gas. The ratios of CO_2 to H_2 gas in the mixtures are 0.05, 0.15, and 0.30, and these atmospheres are symbolized throughout this paper by H_2-5CO_2, H_2-15CO_2, and H_2-30CO_2, respectively. The atmosphere in the cooling-down stage was always pure hydrogen, independent of previous sintering atmospheres.

The mixture of hydrogen and carbon dioxide constituting a sintering atmosphere reacts in thermodynamic equilibrium at elevated temperatures as follows :

$$CO_2 + H_2 \rightarrow CO + H_2O$$

$$H_2O \rightarrow H_2 + \frac{1}{2} O_2$$

The resultant composition of these gases is determined by the equilibrium constant, which is a function of the temperature of gases. The SOLGASMIX program [7] was used to calculate the oxygen potential of sintering atmospheres, which is shown as a function of the temperature in Fig. 2. The oxygen potential increases with the ratio of CO_2 to H_2 gas in the sintering atmosphere and the oxygen potential used in this work ranges from -400 kJ/mole to -300 kJ/mole. The oxygen potential of fuel material is adjusted to reach the equilibrium with that of the sintering atmosphere.

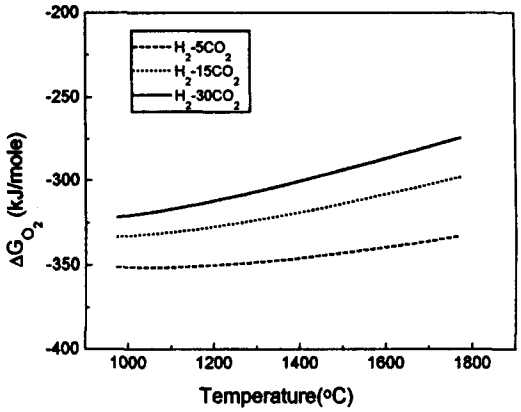

Fig. 2. Oxygen Potential of H_2-CO_2 Mixed Gases

However, the equilibrium may not be perfectly achieved during sintering, especially in a heating stage, since it needs a considerable time even at a fixed temperature.

Sintered density and open porosity were determined from the following relations between dry weight, suspension weight in water, and impregnated weight of sintered pellets [8] :

$$\text{sintered density} = \rho_{pellet} = \frac{W_{dry}}{W_{imp} - W_{sus}} \rho_x$$

$$\text{open porosity} = P_{op} = \frac{W_{imp} - W_{dry}}{W_{imp} - W_{susp} - W_{dry}\frac{\rho_x}{\rho_{TD}}} \times 100, \%$$

where,

ρ_{pellet} : sintered density of pellet,
P_{op} : ratio of open porosity to total porosity
W_{dry} : dry weight,
W_{imp} : impregnated weight,
W_{susp} : suspended weight
ρ_x : density of water,
ρ_{TD} : theoretical density of pellet = $10.962 - 3.485 \times 10^{-2} \cdot$ (wt% of Gd_2O_3) [2].

Sintered pellets were sectioned longitudinally

Fig. 3. SEM Micrographs of UO_2 Powders
(a) AUC-UO_2 powder,
(b) ADU-UO_2 powder

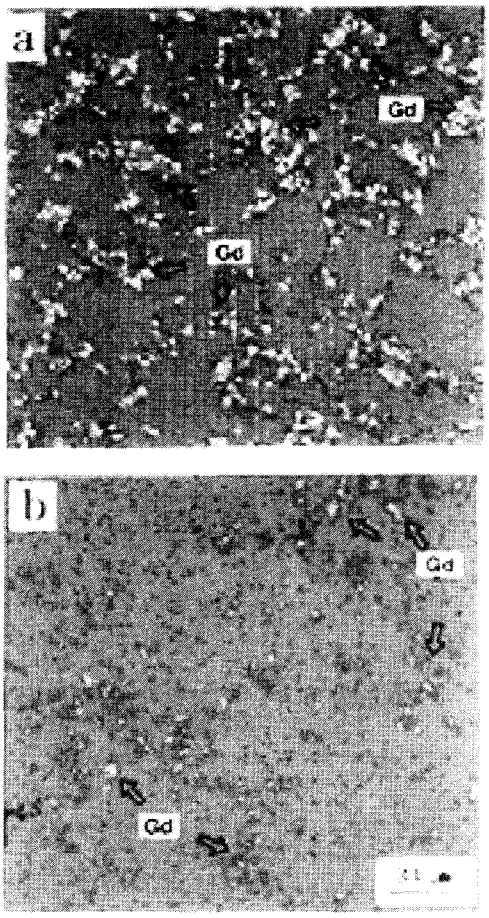

Fig. 4. Area Mapping of Gd Distribution in Green Pellets
(a) powder type I,
(b) powder type II

and polished. Microstructure was observed with OM and SEM, and gadolinium distribution was analyzed by EPMA attached to SEM. To disclose grain boundary thermal etching was carried out at 1250℃ for 1 hour in carbon dioxide atmosphere. Grain size was determined by a linear intercept method, in which about 300 intercepts were counted. Lattice parameters of $(U,Gd)O_2$ solid solutions were determined by X-ray diffraction. Sintered pellets were broken into particulates, and then X-ray diffraction was conducted with monochromatic Cu-K radiation. Diffraction angles (2θ) larger than 60° were considered in calculating lattice parameters.

3. Results and Discussion

Morphologies of AUC-UO_2 and ADU-UO_2 powders are shown in Fig. 3(a) and 3(b), respectively. The AUC-UO_2 powder has a round shape and smooth surface. Its particle size is about 20㎛. When examining the surface of a particle with higher magnification, a particle is composed of fine crystallites and a lot of micropores are present between

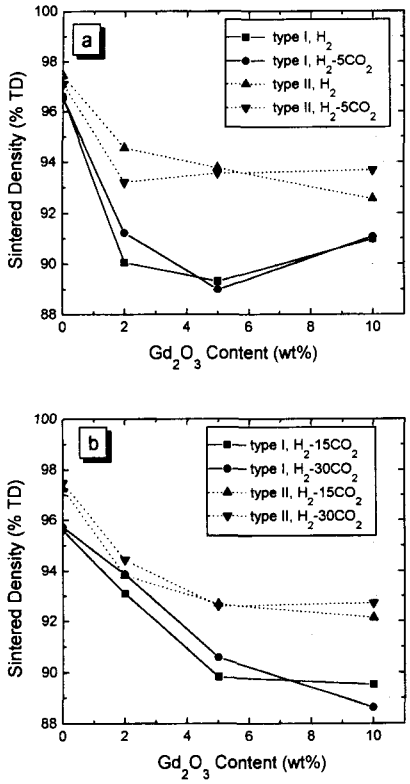

Fig. 5. Sintered Density of UO_2-Gd_2O_3 Pellets as a Function of Gd_2O_3 Content (a) H_2 and H_2-5CO_2 Atmospheres, (b) H_2-15CO_2 and H_2-30CO_2 Atmospheres

crystallites. The ADU-UO_2 powder is much agglomerated and the agglomerates seem to have very irregular sizes.

Gadolinium was analyzed in the green pellet containing 10 wt% Gd_2O_3, of which area mapping are shown in Figs. 4(a) and 4(b). In the green pellet of powder type I (see Fig. 4(a)), it can be seen that Gd is situated between round UO_2 particles and in addition some large Gd agglomerates are formed. In the green pellet of powder type II (see Fig. 4(b)), relatively small Gd agglomerates are found and these agglomerates seem to be concentrated or depleted in some areas. Comparing Fig. 4(a) with Fig. 4(b), Gd agglomerates seem to be

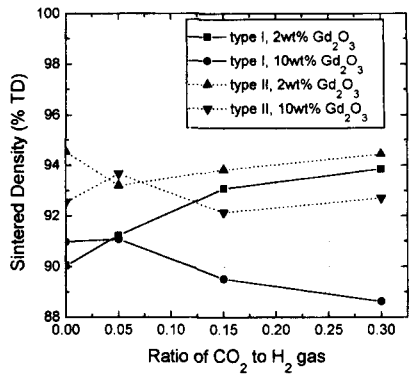

Fig. 6. Dependence of Sintered Density on Oxygen Potential

more locally present and also to be larger in the green pellet of powder type I than in that of powder type II.

Figs. 5(a) and 5(b) show the effect of Gd_2O_3 contents and powder types on sintered density. Sintered densities of the pure UO_2 fuel using AUC-UO_2 powder are lower by about 1 to 1.5 %TD than those using ADU-UO_2 powder, but the density difference between two powder types becomes much larger in UO_2-Gd_2O_3 fuel pellets, indicating that the addition of Gd_2O_3 inhibits densification more in powder type I than in powder type II. Fig. 5(a) shows that the addition of 2 wt% Gd_2O_3 decreases the sintered density substantially and larger addition has a small effect. Such a variation in density is in good agreement with other literatures [9,10]. This dependence of sintered density on the Gd_2O_3 content is found for both powder types in H_2 and H_2-5CO_2 atmospheres. On the other hand, Fig. 5(b) shows that sintered densities decrease gradually with the Gd_2O_3 content for both powder types in H_2-15CO_2 and H_2-30CO_2 atmospheres. Conse-quently, it is thought that the densification of UO_2-Gd_2O_3 fuel pellet is influenced by powder type and oxygen potential.

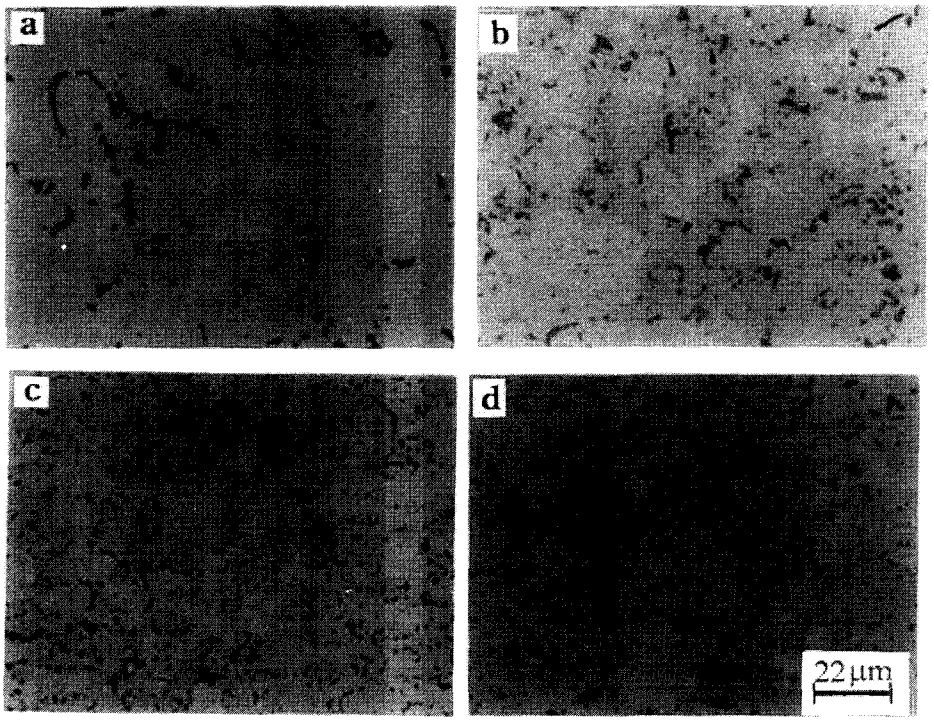

Fig. 7. Pore Structures of Sintered UO_2-10wt% Gd_2O_3 Pellets of Powder Type I
(a) H_2, (b) H_2-5CO_2, (c) H_2-15CO_2, (d) H_2-30CO_2

Fig. 6 shows the effect of oxygen potential on the sintered density of UO_2-Gd_2O_3 pellets. The density of UO_2-2wt% Gd_2O_3 pellet increases with the ratio of CO_2 to H_2 gas, but that of UO_2-10wt% Gd_2O_3 pellet decreases. Such behaviors are prominent in powder type I but are slight in powder type II.

If Gd ions enter UO_2 lattice, defects should be formed in order to fulfill the condition of charge neutrality. Ho and Radford [2] discussed the formation of defects in reducing and oxidizing atmospheres. In a reducing atmosphere the substitution of Gd^{3+} for U^{4+} probably yields an oxygen vacancy in the UO_2 lattice ;

$$Gd_2O_3 \xrightarrow[2UO_2]{} 2Gd'_U + 3O_O + V_O^{\cdot\cdot} \quad (1)$$

This increase in concentration of the oxygen vacancy diminishes the concentration of uranium vacancies through Schottky equilibrium, and thus retards the material transport depending on uranium vacancies. On the other hand, the substitution of Gd^{3+} for U^{4+} probably yields U^{5+} in an oxidizing atmosphere ;

$$Gd_2O_3 + \frac{1}{2}O_2(g) \xrightarrow[2UO_2]{} 2Gd'_U + 2U_U^{\cdot} + 4O_O \quad (2)$$

The formation of U^{5+} can facilitate uranium diffusion since the size of U^{5+} (0.88 Å) is smaller than that of U^{4+} (1.00 Å). Consequently, it is postulated that an oxidizing atmosphere can enhance the densification of

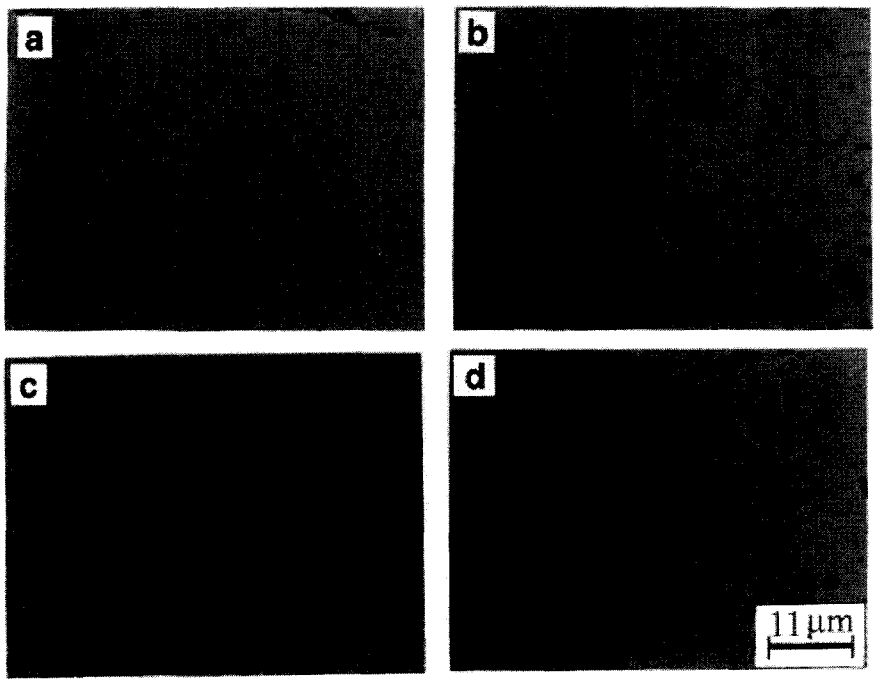

Fig. 8. Grain Structures of Sintered UO_2-5wt% Gd_2O_3 Pellets of Powder Type I
(a) H_2, (b) H_2-5CO_2, (c) H_2-15CO_2, (d) H_2-30CO_2

UO_2-Gd_2O_3 pellets by means of the faster uranium diffusion. This postulation explains the dependence of the sintered densities of UO_2-2wt% Gd_2O_3 pellets on the oxygen potential but does not agree with the decrease in sintered density for UO_2-10wt% Gd_2O_3 pellets.

The decrease in sintered density was found under high oxygen potential in other works [3,11]. Yuda and Une[3] reported that the density began to decrease above specific oxygen potential, which was dependent on Gd_2O_3 content ; -280 kJ/mole for 5 wt% Gd_2O_3 and -330 kJ/mole for 10 wt% Gd_2O_3. In Fig. 6 the sintered density of UO_2-10wt% Gd_2O_3 pellets begins to decrease in the H_2-5CO_2 atmosphere of which oxygen potential is -371 kJ/mole at the sintering temperature (1680℃). This value is comparable to that determined by Yuda and Une.

The decrease in density due to oxygen potential occurs significantly in the UO_2-10 wt% Gd_2O_3 pellets of powder type I (see Fig. 6). The pore structures of these pellets in various oxygen potentials are shown in Figs. 7(a) to 7(d). It is found that the number of pores increases as the oxygen potential increases. Comparing Fig. 7(c) with Fig. 7(d), pore growth seems to occur considerably. The formation of new pores is likely to be the main reason for the decrease in density. The same phenomena were observed by Yuda and Une [3], who supposed that the sintering between UO_2 and UO_2 particles rapidly progressed prior to the sintering between UO_2 and Gd_2O_3 particles under high oxygen potential and thus large closed pores were formed just near Gd_2O_3 particle by the shrinkage of UO_2 particles. The above supposition implies that the sintering

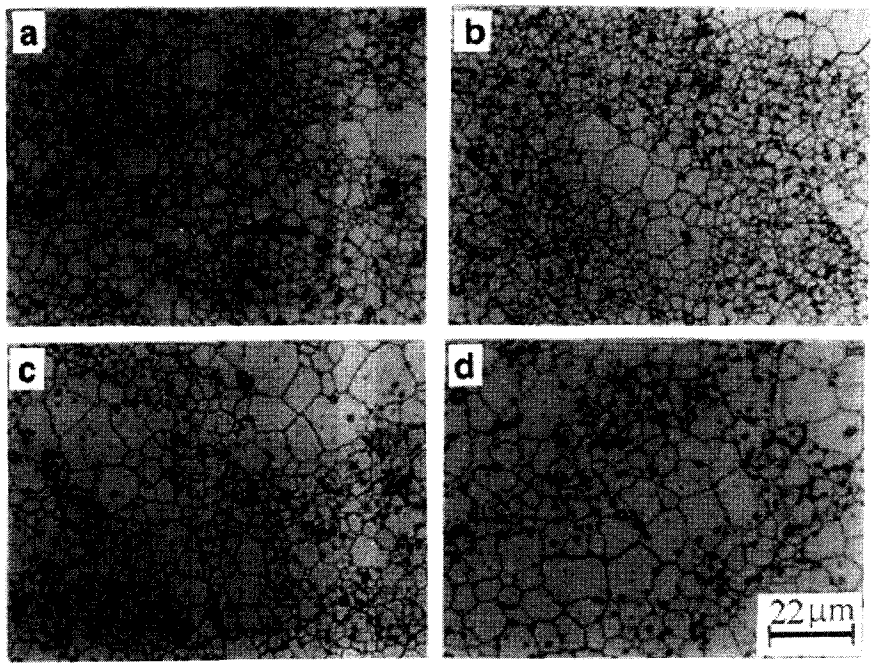

Fig. 9. Grain Structures of Sintered UO_2-5wt% Gd_2O_3 Pellets of Powder Type II
(a) H_2, (b) H_2-5CO_2 , (c) H_2-15CO_2 , (d) H_2-30CO_2

between UO_2 and Gd_2O_3 particles progresses less under high oxygen potential. However, as will be shown in Fig. 11, Gd distribution becomes more homogeneous as oxygen potential increases, which means that the reaction between UO_2 and Gd_2O_3 particles occurs easily under high oxygen potential. So the mechanism of pore formation under high oxygen potential has not been fully understood.

Figs. 8(a) to 8(d) show the grain structures of UO_2-5wt%Gd_2O_3 fuel in various sintering atmospheres for powder type I. Figs. 9(a) to 9(d) show the grain structures of the same condition for powder type II. The grain structure is relatively homogeneous for powder type I, but the grain structure is not homogeneous for powder type II. Some areas have large grains and the other areas have very small grains. Such inhomogeneity tends to be mitigated as the oxygen potential increases.

Fig. 10 shows the line profile of Gd across the inhomogeneous grain structure for powder type II. Gd concentration is high in the area of small grains but low in the area of large grains. As shown in Fig. 4(b), small Gd agglomerates are concentrated or depleted in some areas for the green pellet of powder type II. These Gd agglomerates may dissolve during sintering in the Gd-concentrated areas, where the grain size is small. So the inhomogeneity in grain structure of sintered pellet seems to be derived from that of the green pellet. According to Nishida and Yuda[11], Gd ions diffuse only 5㎛ for 4 hours at 1750℃. It is reasonable to suppose that Gd ions do not diffuse such a long distance during sintering that the inhomogeneity in the green pellet disappears entirely in the sintered pellet. Thus it is inferred that the Gd homogeneity over of the long distance (range) is determined by powder type

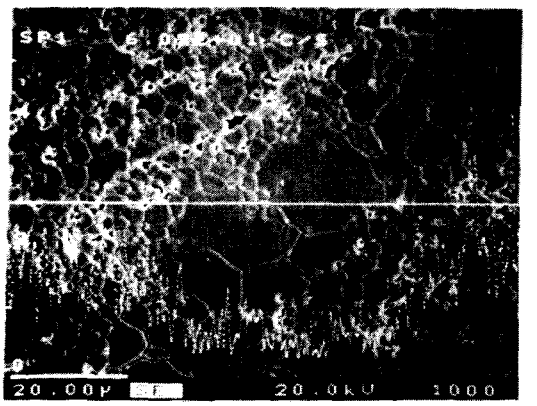

Fig. 10. Variation in Gd Concentration Across Inhomogeneous Grains (Powder Type II)

or powder mixing rather than by sintering.

The line profile of gadolinium (Gd) concentration was analyzed with EPMA and shown in Fig. 11(a) and 11(b) for the UO_2-10wt% Gd_2O_3 pellets of sintered in hydrogen and H_2-30CO_2 atmospheres, respectively. The variation in gadolinium concentration seems to be larger in hydrogen than in H_2-30CO_2 atmosphere. This indicates that high oxygen potential provides a favorable condition for uniform $(U,Gd)O_2$ solid solution. According to the Eqs. (1) and (2), the oxygen vacancy and the U^{5+} ion may be formed in reducing and oxidizing atmospheres, respectively. Since the formation of the oxygen vacancy leads to the decrease in the number of uranium vacancy, Gd ions diffuse very limitedly in a reducing atmosphere. The number of uranium vacancy may not decrease in an oxidizing atmosphere, so Gd ions can diffuse more. Therefore, the Gd homogeneity over a short range can be enhanced by increasing oxygen potential.

Fig. 12 shows the dependence of the grain size of UO_2-Gd_2O_3 pellets on the ratio of CO_2 to H_2 gas in the sintering atmospheres for powder type I. The grain size increases substantially and then remains nearly constant

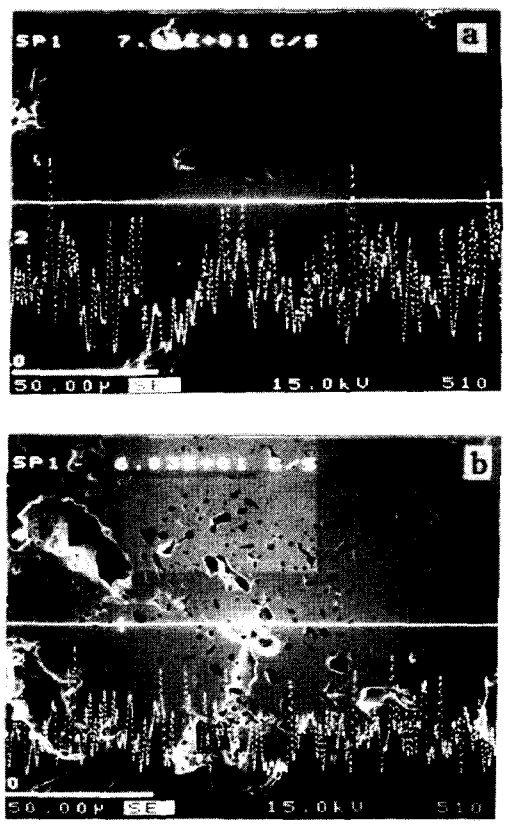

Fig. 11. Line Profile of Gd Concentration in Sintered UO_2-10wt% Gd_2O_3 Pellets from Powder Type I
(a) H_2 , (b) H_2-30CO_2

as the ratio of CO_2 to H_2 gas increases. The grain size decreases with increasing Gd_2O_3 content. This trend is in good agreement with other published works [3,11], and can be explained in terms of the change in stoichiometry and the structural inhomogeneity. The $(U,Gd)O_2$ solid solution has a higher oxygen potential than pure UO_2, so it is more subject to being in a hypostoichiometric state under H_2 atmosphere than pure UO_2. In hypostoichiometric state the number of uranium vacancy decreases due to the increase in the number of oxygen vacancy. Thus uranium diffusion will be slower, yielding

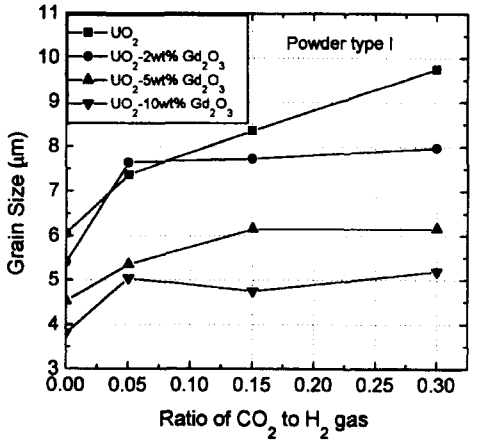

Fig. 12. Grain Sizes of UO_2-Gd_2O_3 Pellets of Powder Type I as a Function of Oxygen Potential

a smaller grain size. The number of uranium vacancy increases under high oxygen potential, and accordingly the grain size increases. The oxygen potential can also influence structural homogeneity of $(U,Gd)O_2$. If Gd concentration is not homogeneous, indissolved Gd particles and the interface between $(U,Gd)O_2$ solid solutions with different Gd concentrations will act as a barrier to the movement of grain boundary. Such inhomogeneity diminishes under high oxygen potential, which can promote grain growth.

Figs. 13(a) and 13(b) show the diffraction patterns of (220) and (311) planes in UO_2-15wt% Gd_2O_3 pellets of powder type I sintered in hydrogen and H_2-30CO_2 atmospheres, respectively. The diffraction pattern in Fig. 13(a) shows a doublet peak consisting of a small peak of UO_2 and a broad peak of $(U,Gd)O_2$, but a single peak of $(U,Gd)O_2$ is found in Fig. 13(b). It is also found that the peaks of $(U,Gd)O_2$ solid solution in H_2-30CO_2 atmosphere are shifted to lower angles, indicating that $(U,Gd)O_2$ solid solution in H_2-30CO_2 atmosphere has a larger lattice

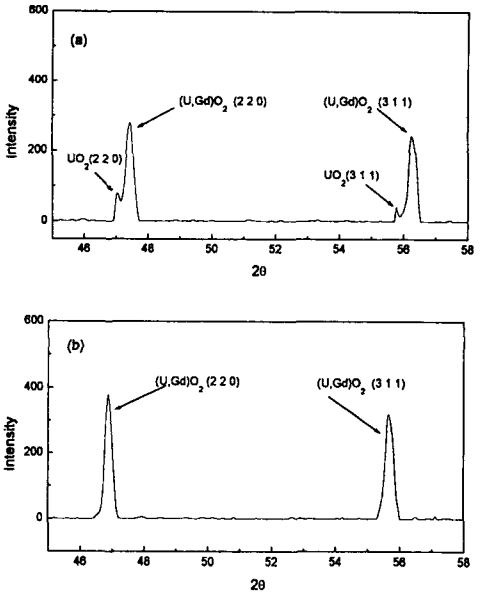

Fig. 13. X-ray Diffraction Patterns of UO_2-15wt% Gd_2O_3 Pellets Sintered in (a) H_2 , (b) H_2-30CO_2

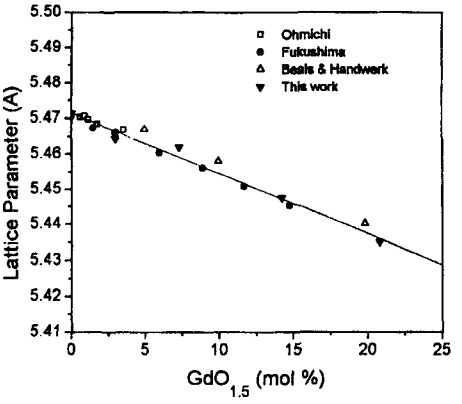

Fig. 14. Lattice Parameters of $(U,Gd)O_2$ Solid Solutions

parameter, and thus contains lower Gd content than the $(U,Gd)O_2$ in hydrogen (see Fig. 14). It can be concluded that the UO_2-15wt% Gd_2O_3 pellet sintered in hydrogen is inhomogeneously composed of pure UO_2 and the $(U,Gd)O_2$ solid solution containing more than 15 wt% of

Gd_2O_3.

Fig. 14 shows lattice parameters of the UO_2-Gd_2O_3 pellets sintered in H_2-30CO_2 atmosphere as a function of the Gd_2O_3 content, together with other published data [12,13,14,15]. The lattice parameter decreases linearly as the Gd_2O_3 content increases, and the correlation between them is as follows :

$$\text{lattice parameter} = 5.4715 - 0.00171 \times (\text{mol \% of } GdO_{1.5}),\ \text{Å}. \quad (3)$$

The decrease in lattice parameter was explained by Ohmichi et al.[12], who proposed that the substitution of Gd^{3+} (1.05Å) for U^{4+} (1.00Å) gave rise to the formation of smaller U^{5+} (0.88Å) and showed that the decreasing rate of the lattice parameter can be well correlated with the reduction in the ionic radius.

4. Conclusions

Sintering characteristics of UO_2-Gd_2O_3 fuel pellets have been investigated in four oxygen potentials and for two powder types, mixing of AUC-UO_2 with Gd_2O_3 powders (type I) and mixing of ADU-UO_2 with Gd_2O_3 powders (type II). Following conclusions can be made:

(1) The addition of Gd_2O_3 lowers the sintered density of UO_2-Gd_2O_3 fuel pellets. This density drop is always larger in powder type I than in the powder type II, and thus the sintered density of UO_2-Gd_2O_3 fuel is dominantly affected by the powder types. As the oxygen potential of sintering atmospheres increases, the density of the UO_2-2wt% Gd_2O_3 pellets increases but that of UO_2-10wt% Gd_2O_3 pellets decreases. This decrease in density seems to be caused by the formation of new pores.

(2) A short range Gd homogeneity is enhanced by increasing oxygen potential, but a long range Gd homogeneity seems to be determined mainly by powder type.

(3) High oxygen potential increases the grain size of UO_2-Gd_2O_3 pellets, mainly because high oxygen potential can generate more uranium vacancies and diminish microstructural inhomogeneity.

(4) A single phase of $(U,Gd)O_2$ solid solution is formed in an oxidizing atmosphere, but pure UO_2 is present in addition to the $(U,Gd)O_2$ solid solution in H_2 atmosphere. The lattice parameter of $(U,Gd)O_2$ solid solution decreases linearly with increasing Gd_2O_3 content.

References

1. R. Manzel, and W.O. Dorr, *Am. Ceram. Soc. Bull.* **59** (1980) 601.
2. S.M. Ho, and K.C. Radfod, *Nucl. Technol.* **73** (1986) 350.
3. R. Yuda, and K. Une, *J. Nucl. Mater.* **178** (1991) 195.
4. H.G. Riella et al. *J. Nucl. Mater.* **178** (1991) 204.
5. H. Assmann and H. Bairiot, "Guide Book on Quality Control of Water Reactor Fuel," IAEA technical series No.221, Vienna, (1983).
6. K.W. Song, D.S. Sohn and W.K. Choo, *J. Nucl. Mater.* **200** (1993) 41.
7. HSC Chemistry for Windows, (1994) Outokump Research.
8. W.O. Doerr et al., *J. Nucl. Mater.* **81** (1979) 135.
9. H. Assmann, M. Peehs and H. Roepenack, *J. Nucl. Mater.* **153** (1988) 115.
10. H.H. Davis, and R.A. Potter, *Mater. Sci. Res.* **11** (1974)515.
11. T. Nishida and R. Yuda, "Effect of particle

size and oxygen potential on UO_2-Gd_2O_3 pellet sintering," IAEA technical committee meeting on Advances in Pellet Technology for Improved Performance at High Burnup, Tokyo, Japan, October, (1996).

12. T. Ohmichi et al., *J. Nucl. Mater.* **102** (1981) 40.
13. J.H. Handwerk, and R.J. Beals, *J. Am. Ceram.* **48** (1965) 271.
14. S. Fukushima and T. Ohmichi, *J. Nucl. Mater.* **105** (1982) 201.
15. R.J. Beals, J.H. Handwerk, and B.J. Wrona, *J. Am. Ceram.* Soc. **54** (1969) 578.